Alkali Metal Oxides, Peroxides, and Superoxides: A Multinuclear MAS NMR Study

Thomas R. Krawietz, David K. Murray, and James F. Haw*

The Center for Catalysis, Department of Chemistry, Texas A&M University, P.O. Box 300012, College Station, Texas 77842-3012

Received: May 20, 1998; In Final Form: July 31, 1998

The many roles of alkali metal−oxygen phases as catalyst components and promoters motivated a survey of the NMR properties of these compounds. Solid state ^{7}Li, ^{23}Na, ^{39}K, ^{87}Rb, and ^{133}Cs magic angle spinning NMR spectra are reported for the following alkali metal oxides, peroxides and superoxides: Li_2O, Li_2O_2, Na_2O, Na_2O_2, NaO_2, KO_2, Rb_2O_2, RbO_2, Cs_2O_2, and CsO_2. Commercial samples labeled as "Cs_2O" proved to be mixtures of Cs_2O_2 and CsO_2. The superoxide (O_2^-) anion is paramagnetic, and this property leads to highly temperature-dependent chemical shifts for the alkali metal nuclei in all of the superoxides. All four superoxides also show phase transitions between polymorphic forms of cubic and lower symmetry, and these transitions profoundly affect the alkali metal NMR spectra. For CsO_2 and RbO_2, purely ionic bonding restricts the paramagnetic shift to the through-space dipolar mechanism, and large temperature-dependent shifts in the tetragonal phases vanish upon transition to the cubic phases. ^{13}C in situ MAS NMR experiments show that the oxide (M_2O) compounds react as bases while the peroxides and superoxides are both bases and oxidizers. Possible roles for peroxide and superoxide phases should be considered for catalysts formulated using alkali metals, especially cesium.

Introduction

Alkali metals are important components in a diverse range of catalytic materials. These elements serve as promoters on supported metal oxidation catalysts, as strongly basic sites for olefin isomerization, and as cations exchanged into zeolites to modify acid−base properties.[1−9] Small alkali metal oxide clusters enclosed within microporous materials may function as "super-basic" sites.[10] Although some workers clearly understand the complex phase diagrams of the alkali metal−oxygen systems, alkali metal oxides in catalytic systems are sometimes represented as M_2O, and this is frequently an oversimplification.

The oxide phases of the alkali metals are reviewed in monographs[11,12] and comprehensive texts on inorganic chemistry.[13] The phase diagrams increase in complexity as one descends the periodic table. In general, the changes between elements are incremental as one descends the group, but there is a significant change between Na and K. Lithium oxide, Li_2O, is the most important oxide of lithium, but the peroxide, Li_2O_2, is readily formed by the reaction of metal and hydrogen peroxide. Lithium superoxide, LiO_2, is stable below 223 K.[14] Na_2O can be prepared by heating the metal with a limiting amount of oxygen, while excess oxygen affords Na_2O_2. Sodium superoxide, NaO_2, can be prepared from Na_2O_2 at high temperature and pressure, as well as by direct reactions of the elements in liquid ammonia. Sodium ozonide, NaO_3, is metastable,[15] and ozonides have also been prepared for the heavier alkali metals.[16] The oxidation of potassium usually forms mixtures of peroxide and superoxide phases, but the oxide has also been reported.[12] Neither Rb nor Cs yields M_2O by direct oxidation of the metal, and if formed, M_2O species readily disproportionate. We show here that commercial samples labeled as "Cs_2O" in fact do not contain any alkali metal oxide but are mixtures of peroxide and superoxide. The complexity of the cesium−oxygen system is further compounded by the existence of a number of suboxides, i.e., Cs_xO_y ($x < y$).[17,18] A sesquioxide, Cs_2O_3, has also been reported;[19] this is probably a mixed phase containing peroxide and superoxide anions. The diversity of oxide phases described above suggests interesting possibilities for stoichiometric or catalytic reactions of alkali metal oxide clusters or phases. Most phases have some degree of basicity, and oxidation chemistry is plausible for the peroxide and superoxide phases.

Solid-state NMR methods have been applied with great success to the study of the structure and function of heterogeneous catalytic materials,[20] and each alkali metal has one or more NMR-active isotopes. In the present investigation, we survey for the first time the NMR properties of the common oxide phases of the alkali metals to lay the groundwork for future studies of actual catalytic materials. All of the nuclei examined, ^{7}Li, ^{23}Na, ^{39}K, ^{87}Rb, and ^{133}Cs, are noninteger quadrupoles, and the central transitions ($m_I = +1/2 \leftrightarrow -1/2$) of such nuclei are not broadened by the quadrupolar interaction to first order. Most of the compounds studied have cubic site symmetry in one or more of the phases studied (particularly the high-temperature phases relevant to catalysis), and the quadrupole coupling constant is exactly zero in these cases. Where the crystal site symmetry is less than cubic, e.g., Cs_2O_2, the use of a moderate field strength (8.45 T) ensures that the observed resonance frequency is primarily due to chemical shift and not quadrupolar effects. We were thus able to survey the NMR properties of these materials using magic-angle spinning as the only line-narrowing technique. The superoxide anion is paramagnetic, and the alkali metal NMR of the all of the superoxides displayed dramatic temperature dependencies in their resonance frequencies. In the case of CsO_2, we are able

* To whom correspondence should be addressed.

10.1021/jp9823190 CCC: $15.00
Published on Web 10/09/1998

to assign this to a dipolar mechanism that produces large shifts in the tetragonal phase but no shift in the cubic phase.

Experimental Section

Materials. Lithium peroxide (technical grade, 90%), sodium peroxide (97%), potassium superoxide (96+%), "Rb_2O" (technical grade, 99+% Rb), sodium metal (99+%), cesium metal (99.5+%), and RbCl (99+%) were purchased from Aldrich. LiCl was purchased from Fisher Scientific. NaCl (99+%) and KCl (99+%) were purchased from EM Science. CsCl (99.96+%) was purchased from Cabot. "Cs_2O" was purchased from Strem, Aldrich, and Alfa Aesar. Ammonia and oxygen gases were purchased from Matheson.

Sodium superoxide was synthesized by rapidly bubbling oxygen through a solution of sodium metal dissolved in anhydrous liquid ammonia.[21] A 330 mL quantity of ammonia was condensed into a 500 mL round-bottom flask immersed in a dry ice/acetone bath, and the flask was connected to a vacuum line. The ammonia was purified by 0.20 g of sodium metal placed in the flask previously. The anhydrous ammonia was then transferred in the vacuum line to another 500 mL flask containing 0.80 g of sodium metal. Oxygen gas was rapidly bubbled through the solution at 198 K, and the system was allowed to warm to room temperature after the deep blue color had completely faded. The flask was evacuated overnight at room temperature to remove any traces of ammonia or oxygen gas.

Cesium peroxide was prepared by the dropwise addition of cesium metal to a mixture of cesium superoxide and cesium peroxide under an anhydrous/anaerobic atmosphere. A red flame was observed in the reaction vessel upon addition of the cesium metal. The vessel was cooled, sealed, and evacuated on a vacuum line, after which, the mixture was heated to 523 K for 4 h. The product was chipped from the reaction vessel, ground, and reheated under vacuum twice more to provide a uniform, charcoal-black material. Multiple trial neutron activation analysis of the oxygen content provided an empirical formula of $CsO_{1.09}$.

All materials were stored in a rigorously anhydrous and anaerobic environment and were sealed into MAS sample rotors immediately prior to spectroscopic observation.

NMR Spectroscopy. ^{7}Li, ^{23}Na, ^{39}K, ^{87}Rb, and ^{133}Cs MAS NMR spectra were obtained on a Chemagnetics CMX-360 spectrometer. All spectra were externally referenced to 0 ppm using 0.1 M LiCl, 0.1 M NaCl, 0.1 M KCl, 0.5 M RbCl, and 0.5 M CsCl, respectively, as standards. ^{7}Li, ^{23}Na, ^{87}Rb, and ^{133}Cs MAS NMR spectra were acquired using a home-built transmission-line probe spinning a 5.0 mm o.d. zirconia rotor. ^{39}K MAS NMR measurements were performed using a highly modified triple resonance probe purchased from Otuska Electronics that spun 7.5 mm o.d. zirconia rotors. All spectra presented were obtained using active spin speed control, and all reported spectra were excited using 10−15° flip angles with the exception of those acquired as echoes. ^{7}Li spectra of Li_2O and ^{23}Na spectra of Na_2O were acquired as quadrupole echoes, while ^{39}K spectra of KO_2 were acquired as spin echoes in order to eliminate probe ringing.

The reported chemical shifts are the "apparent" values obtained at a field strength of 8.45 T and have not been corrected for the quadrupolar shift. T_1 measurements used either the inversion−recovery or the saturation−recovery sequence. At least eight relaxation times were used for each T_1 determination, and these were fit using a least-squares routine.

TABLE 1: ^{7}Li, ^{23}Na, ^{39}K, ^{87}Rb, and ^{133}Cs NMR Properties

nuclide	ν_0 (MHz)[a]	I	Q (barn)[b]	natural abundance (%)[b]
^{7}Li	139.81	$^{3}/_{2}$	-4×10^{-2}	92.58
^{23}Na	95.157	$^{3}/_{2}$	1.0×10^{-1}	100
^{39}K	16.787	$^{3}/_{2}$	4.9×10^{-2}	93.1
^{87}Rb	117.71	$^{3}/_{2}$	1.3×10^{-1}	27.85
^{133}Cs	47.184	$^{7}/_{2}$	-3×10^{-3}	100

[a] Resonance frequency, ν_0, with ^{1}H at 359.73 MHz. [b] Taken from ref 38.

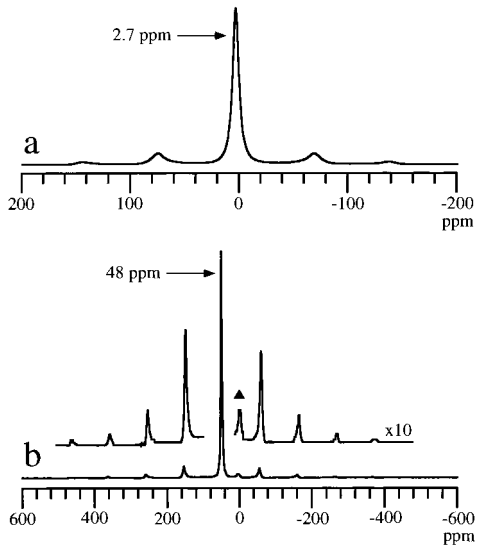

Figure 1. ^{7}Li and ^{23}Na MAS NMR spectra of (a) Li_2O and (b) Na_2O. Both spectra were acquired using a quadrupole echo pulse sequence at 303 K and a spinning speed of 10 kHz. The ^{7}Li MAS spectrum is the result of 4 transients utilizing a 60 s recycle delay. The ^{23}Na MAS spectrum is the result of 64 transients and a 10 s recycle delay.

X-ray Diffraction. X-ray powder diffraction patterns of alkali metal peroxides and superoxides were obtained using a Seifert-Scintag PAD V automated diffractometer with Cu $K\alpha_1$ radiation. Samples were loaded into forms in a glovebox, covered with a 30 μm thick Mylar packing tape film, and analyzed immediately afterward. The X-ray source was an anode operating at 40 kV and 30 mA with a copper target, and the radiation was filtered with nickel foil ($\lambda = 1.5418$ Å). Data were collected between 5 and 62° in 2θ with a step size of 0.04° and a scan rate of 2°/min. The measured X-ray diffraction patterns were compared with those reported in the JCPDS database.

ESR Spectroscopy. Weighed ground samples (0.7−0.9 g) known or suspected to contain superoxide phases were loaded into 4 mm i.d. quartz ESR tubes in a drybox and then evacuated with mild vacuum. X-band (9.4 GHz) ESR spectra were obtained with a Bruker ESP 300 spectrometer. All spectra were measured at 100 K. Quantitation of superoxide anion content was performed by integration of spectra phased in the absorption mode and comparison to either 99% potassium superoxide or 0.0010 M aqueous cupric sulfate.

Results

For the convenience of the reader, the NMR properties of the various nuclei studied are collected in Table 1. The results are reported by anion in order of increasing formal oxidation state for oxygen.

Alkali Metal Oxides. Figure 1 shows the ^{7}Li MAS spectrum of Li_2O and the ^{23}Na MAS spectrum of Na_2O. Both oxides belong to space group $Fm3m$ with one cation per unit cell, and

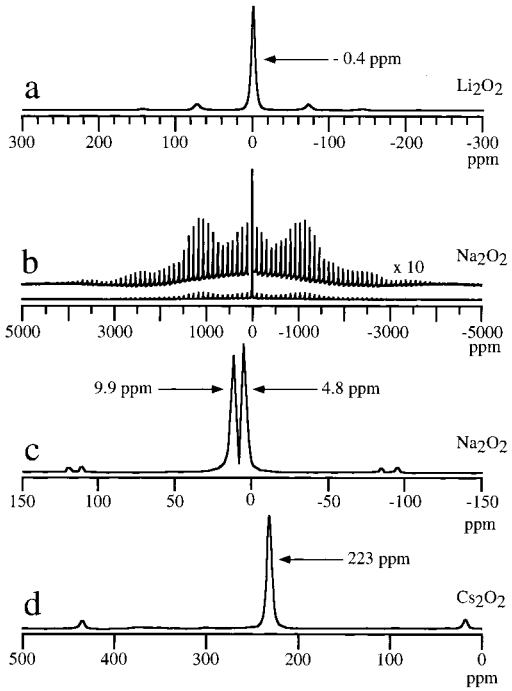

Figure 2. ^{7}Li, ^{23}Na, and ^{133}Cs MAS NMR spectra of (a) Li_2O_2, (b, c) Na_2O_2, and (d) Cs_2O_2. The spectrum shown in (c) is an enlargement of the region surrounding the central transition of Na_2O_2, resolving the two crystallographically distinct sodium sites. All spectra were acquired with a spinning speed of 10 kHz.

this is reflected in the single resonance in each spectrum. There are reports of K_2O in the literature, but we were unable to locate a commercial source of this compound. We made a number of attempts at the preparation of Cs_2O, but without obvious success. These efforts included heating cesium hydroxides, peroxide, or superoxide in vacuo; in some cases, we obtained poorly defined materials with unique ^{133}Cs resonances, but none of these materials had empirical formulas near Cs_2O.

Alkali Metal Peroxides. Figure 2 shows the ^{7}Li, ^{23}Na, and ^{133}Cs MAS NMR spectra of Li_2O_2, Na_2O_2, and Cs_2O_2. Each of these compounds was characterized by X-ray powder diffraction and elemental analysis and was determined to be of high purity. Li_2O_2 belongs to the hexagonal space group $P\bar{6}$ and contains two crystallographically distinct lithium cations located in sites of 3-fold symmetry.[22] These are not resolved in Figure 1a, and this is not surprising in view of the small chemical shift range for lithium. The existence of two sites was reflected in the spin−lattice relaxation behavior of the Li_2O_2 resonance; the return to equilibrium exhibited a biexponential decay of equal populations.

Na_2O_2 belongs to the hexagonal space group $P\bar{6}2m$, which is different from the space group of the lithium compound, but Na_2O_2 also has two unique cations in 3-fold sites. The larger chemical shift range and larger quadrupole moment of ^{23}Na are reflected in the spectrum of sodium peroxide (Figure 2b and expanded view in Figure 2c). Expansion of the area immediately surrounding the central transition (Figure 2c) reveals the crystallographically distinct sites at 9.9 and 4.8 ppm.

Figure 2d shows the ^{133}Cs MAS NMR spectrum of Cs_2O_2. A single, narrow resonance is observed at 223 ppm. This is consistent with the crystal structure, which shows one unique cation site.[22] Figure 2d also illustrates the very large chemical shift range of ^{133}Cs NMR and the fact that narrow spectral lines are often obtained with crystal site symmetry well below cubic (the space group of Cs_2O_2, *Immm*, is orthorhombic).

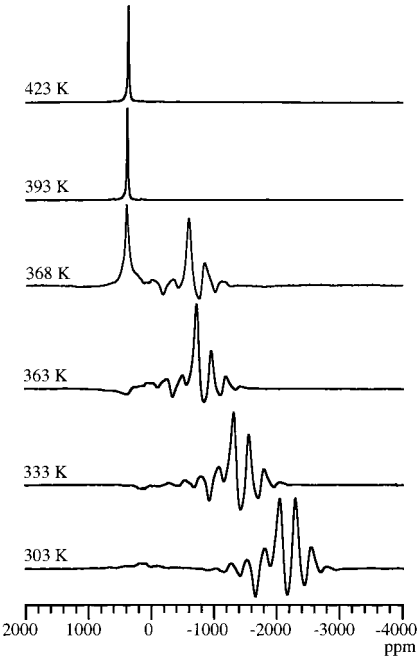

Figure 3. Variable-temperature ^{133}Cs MAS NMR spectra of CsO_2. At temperatures below 368 K, CsO_2 exists as α-CsO_2 and shows a strongly temperature-dependent chemical shift. At 368 K, α-CsO_2 reversibly converts to β-CsO_2. The ^{133}Cs shift is not temperature-dependent for this polymorph. Each spectrum is a result of 1024 transients, a 1 s recycle delay, and a spinning speed of 10 kHz. Line shape distortions reflect the rapid decay of the FID during the finite (9 μs) receiver delay. A small amount of diamagnetic Cs_2O_2 is seen near 223 ppm.

Alkali Metal Superoxides. The superoxide anion is paramagnetic, and paramgnetism introduces many complexities and opportunities in MAS NMR, especially temperature-dependent shifts. The presence of superoxide anions in these compounds was established unambiguously by observation of the ESR signal for this species and comparison to that of an authentic sample of KO_2. ESR proved valuable as an adjunct to elemental analysis in our synthesis and characterization of samples of high-purity CsO_2.

Not surprisingly, NMR characterization of the superoxides required a substantially greater effort than that of the oxides and peroxides. We characterized CsO_2, RbO_2, KO_2, and NaO_2; each compound presented unique challenges as a result of different crystal phases and crystal phase transitions compounded by the varied NMR properties of the alkali metal nuclei (Table 1). Once understood, the results for CsO_2 were straightforward, but this compound was initially challenging. We purchased materials sold and labeled as "Cs_2O" from several vendors. In every case, these materials were actually mixtures of CsO_2 and Cs_2O_2. Furthermore, the CsO_2 signal is resolved only at higher temperatures (vide infra) or with high-speed MAS, and the samples of "Cs_2O" initially gave anomalous spectra in which the spin count of the Cs_2O_2 signal at 223 ppm and its spin−lattice relaxation behavior varied widely. Once we recognized that "Cs_2O" was a mixture of peroxide and superoxide, it became apparent that the NMR properties of the diamagnetic Cs_2O_2 in these samples varied with the amount of CsO_2 and the intimacy of mixing.

CsO_2 is known to have two crystallographic phases; α-CsO_2 (tetragonal, *I*4/*mmm*) exists below ca. 368 K, and β-CsO_2 (cubic, *Fm*3*m*) exists above this temperature. The ^{133}Cs observables of CsO_2 dramatically reflect this phase transformation. The ^{133}Cs spectra in Figure 3, obtained with 10 kHz magic angle spinning (MAS), are representative of the results obtained for

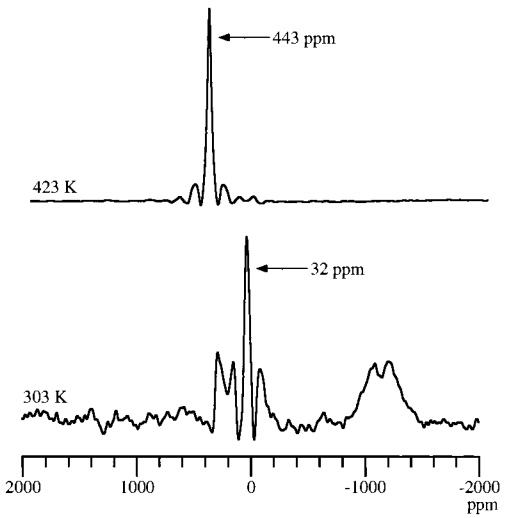

Figure 4. ^{87}Rb MAS NMR spectra of a mixture of Rb_2O_2 and RbO_2. At 303 K, Rb_2O_2 and α-RbO_2 are observed at 32 and ca. −1100 ppm, respectively. At 423 K, β-RbO_2 is observed at 443 ppm. Each spectrum is a result of 1024 transients, a 1 s recycle delay, and a spinning speed of 10 kHz.

CsO_2 samples from various sources or preparations. One notes a single resonance (and associated spinning sidebands) at a chemical shift that is highly temperature dependent. We measured the chemical shift of this signal between 98 K (where its line width is 280 kHz) and 368 K, where it abruptly but reversibly gives way to a signal at 403 ppm with no measurable temperature dependence. Nonspinning spectra (not shown) confirm an axially symmetric shift tensor for the low-temperature phase, as required by cesium's 4-fold site symmetry, and a completely symmetric tensor for the high-temperature phase, as required by cubic symmetry. Recycle delays were used such that the resonance of cesium peroxide was suppressed in order to simplify the observed spectra. Traces of the cesium peroxide can be seen at ca. 223 ppm; vide supra. The line shape distortions in Figure 3 are a result of the finite receiver delay of the spectrometer. Rotor-synchronized echo-type sequences were attempted to rectify the problem but were unsuccessful due to complete loss of signal during echo defocusing and refocusing periods. The ^{133}Cs T_2 of α-CsO_2 was measured using a spin echo on static samples and was found to be 80 μs at 303 K.

Variable-temperature ^{87}Rb MAS NMR spectra of mixtures of Rb_2O_2 and RbO_2 were reminiscent of those for the cesium compounds with the exception that the phase transition temperature for RbO_2 was 408 K, and the quadrupolar interaction (negligible for ^{133}Cs) significantly contributed to the line shape of the ^{87}Rb spectra. Figure 4 presents two ^{87}Rb MAS spectra that summarize the important features of this study. The spectrum recorded at 303 K shows NMR signals with complicated line shapes for both species. The signal with a maximum at 32 ppm is due to Rb_2O_2 and shows little if any temperature dependence. The broad signal near −1100 ppm at 303 K is due to the low-temperature phase of rubidium superoxide (α-RbO_2), and the position of this signal is strongly temperature dependent. The spectrum recorded at 423 K is almost completely dominated by the sharp signal near 443 ppm for the high-temperature phase of rubidium superoxide (β-RbO_2); the signal for Rb_2O_2 is dwarfed in this presentation.

KO_2 has the same crystallographic phase transition between tetragonal (*I*4/*mmm*) and cubic (*Fm*3*m*) polymorphs as CsO_2 and RbO_2, and the variable-temperature ^{39}K rotor-synchronized,

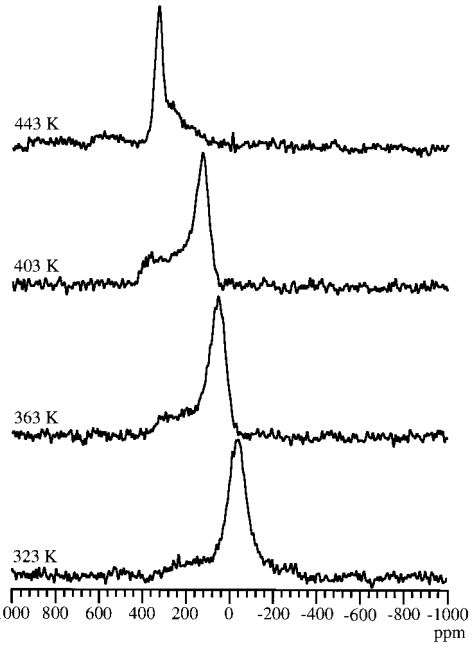

Figure 5. Variable-temperature ^{39}K MAS NMR spectra of KO_2. Below 388 K, α-KO_2 solely exists. Between 353 and 423 K, α-KO_2 and β-KO_2 are observed by ^{39}K MAS NMR. Above 423 K, only β-KO_2 is observed. Both polymorphs exhibit temperature-dependent ^{39}K chemical shifts due to the paramagnetic superoxide anion. Each spectrum is a result of 1024 transients using a 1 s pulse delay. All spectra were acquired using a rotor-synchronized (5 kHz) spin-echo sequence to eliminate probe ringing.

spin-echo MAS NMR spectra of this compound are presented in Figure 5.[23] However, the ^{39}K MAS NMR spectra of KO_2 show two unique characteristics. While the other superoxides have well-defined transition temperatures, α-KO_2 and β-KO_2 coexist between 353 and 423 K, and only above that range is the conversion to β-KO_2 complete. This sluggish transition has been previously noted.[24] Second, the apparent ^{39}K chemical shifts of both phases of KO_2 are temperature dependent.

NaO_2 has three reported polymorphs that are stable over the temperature range studied. NaO_2 (I), a cubic form having a disordered pyrite structure, is stable above 223 K, and like many high-temperature superoxide phases, the superoxide anions have effective spherical symmetry due to rapid reorientation.[25,26] Two lower temperature polymorphs of NaO_2 have been claimed in the literature, and these have been designated as NaO_2 (II) and NaO_2 (III). NaO_2 (II), a second cubic phase having an ordered pyrite structure, is proposed to be stable between 223 and 196 K. The distinction between NaO_2 (I) and NaO_2 (II) is thought to be the extent to which the superoxide groups are able to reorient.[26,27] Below 196 K, NaO_2 (III) is the stable polymorph. It belongs to an orthorhombic space group (*Pnmm*).[26] Figure 6 displays selected variable-temperature ^{23}Na MAS spectra from a detailed study of NaO_2. Our spectra show that a very substantial broadening occurs in the vicinity (i.e., 208 K) of the reported transition temperature to form NaO_2 (III), but the spectra at higher temperatures show little if any evidence of a distinct NaO_2 (II) phase—rather we observe a continuous shift in the ^{23}Na resonance frequency as the temperature is increased between 208 and 348 K. The extreme breadth of the NaO_2 (III) signal precluded a measurement of the temperature dependence of its apparent shift.

Figure 7 summarizes the temperature dependencies of the apparent alkali metal shifts for the four MO_2 compounds studied. These plots demonstrate that high-temperature cubic phases of both CsO_2 and RbO_2 have alkali metal NMR shifts that are

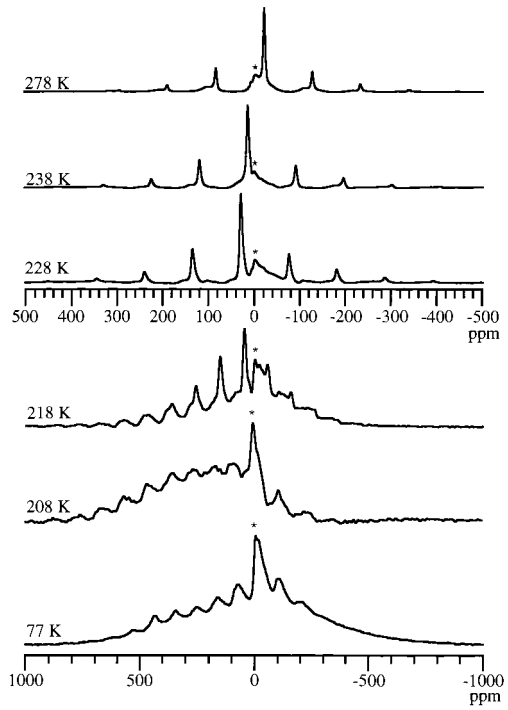

Figure 6. Variable-temperature ^{23}Na MAS NMR spectra of NaO_2. Asterisks denote a Na_2O_2 impurity. Below 198 K, NaO_2 converts to an orthorhombic polymorph and the signal becomes extremely broadened due to the loss of cubic symmetry about the sodium cation. Each spectrum is a result of 256 transients, a 1 s recycle delay, and a spinning speed of 10 kHz.

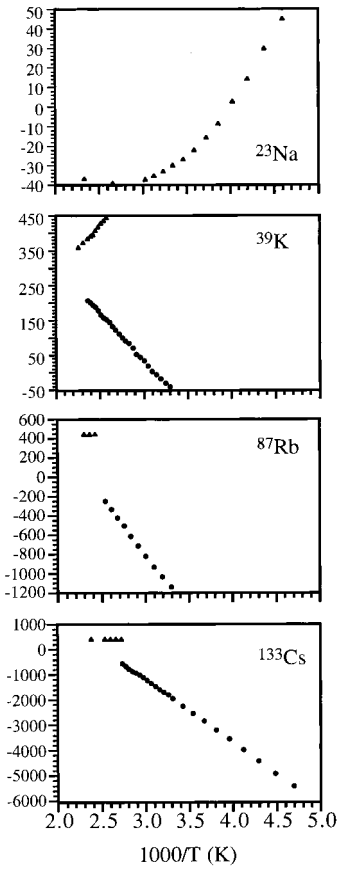

Figure 7. Plots of apparent ^{23}Na, ^{39}K, ^{87}Rb, and ^{133}Cs chemical shifts vs $1/T$ for NaO_2, KO_2, RbO_2, and CsO_2. All measurements were performed with 10 kHz MAS, except for that of ^{39}K which was performed with 5 kHz. The tetragonal and cubic polymorphs are denoted by ▲ and ●, respectively.

temperature independent, while the low-temperature phases show strong Curie law ($1/T$) dependencies. Both KO_2 and NaO_2 show clear temperature dependencies for the apparent shifts in the high temperature phases. Phase transitions are readily apparent in these plots for CsO_2, RbO_2, and KO_2, where they are reflected in discontinuities in both the apparent shift and the first derivative of shift with respect to ($1/T$). In the case of sodium superoxide, we were unable to acquire apparent chemical shift data for the NaO_2 (III) phase, but the transition was apparent in the line widths of the ^{23}Na MAS spectra. We will return to these plots in the discussion of the mechanism of temperature-dependent chemical shifts.

Reaction Chemistry. We used in situ ^{13}C MAS NMR spectroscopy[28,29] to survey the reactivity of many of the compounds discussed here with organic compounds. In general, the simple oxides, M_2O, showed only basic properties while the peroxides and superoxides showed both basic and oxidative reactivity. Figure 8 shows representative results for the reactions of methanol on sodium oxide and sodium peroxide. On Na_2O, methanol is deprotonated to form sodium methoxide, and this is unreactive even at 598 K. The methoxide also forms at 298 K on Na_2O_2, and in Figure 8 we show by a slow-speed MAS spectrum that this species has an axially symmetric chemical shift tensor, as expected. Upon being heated to 523 K, the methoxide is completely oxidized on sodium peroxide to sodium carbonate.

Discussion

The NMR properties of the M_2O and M_2O_2 compounds are straightforward and require little discussion. Both the ^{7}Li and ^{23}Na spectra indicate that the alkali metal nuclei are less shielded for the oxides relative to the peroxides. Unfortunately, NaO_2 exhibits temperature-dependent shifts in all phases, and we are not able to directly compare oxides and peroxides with superoxides for a single alkali metal. For ^{87}Rb and ^{133}Cs, the shifts of the high-temperature superoxide phases are downfield of the corresponding proxide phases. Therefore, a shielding order of $M_2O_2 > M_2O > MO_2$ is suggested.

The differences in chemical properties between the simple oxides, M_2O, and the peroxides and superoxides are noteworthy. Some applications of alkali metals in catalysis involve selective oxidations, and the possibility of peroxide or superoxide species being involved in some alkali-metal-promoted reactions should be considered. Cesium is commonly used as a catalyst component, and if Cs_2O exists at all, it must form under unusual circumstances. Cesium peroxide and cesium superoxide are almost certainly present in some catalyst formulations described as containing "Cs_2O". If not recognized, the broad ^{133}Cs signal from CsO_2 could introduce interpretation problems in NMR studies of catalytic materials. Most NMR spectra are run in the vicinity of 298 K, a temperature at which this resonance lies near −2000 ppm. Since this is well outside the normal range for ^{133}Cs NMR, most workers would not set their sweep widths to include this region, and the resonance of CsO_2 could fold into the spectrum as a broad or poorly phased feature.

The temperature-dependent shifts of the alkali metal superoxides require a detailed discussion. Previous work has characterized temperature-dependent shifts in MAS spectra of ^{13}C,[30−32] ^{89}Y,[33] and ^{119}Sn[34] in paramagnetic solids. Measurements of the complex temperature dependence of the ^{13}C shifts for Cu(II) carboxylate dimers have been quantitatively interpreted in terms of antiferromagnetic superexchange coupling.[35,36]

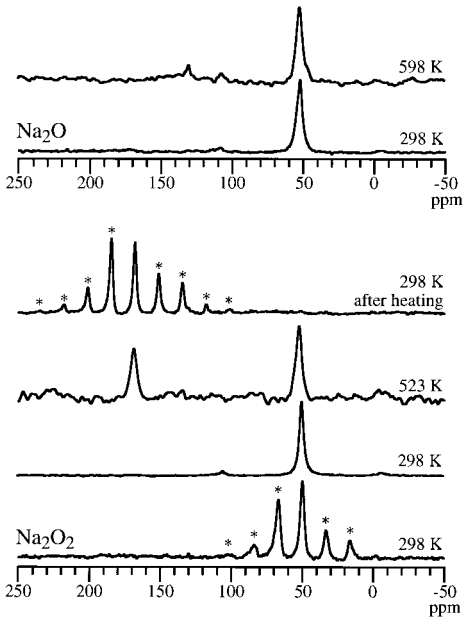

Figure 8. Variable-temperature ^{13}C Bloch decay MAS NMR spectra of methanol-^{13}C adsorbed on Na_2O and Na_2O_2. After adsorption at 298 K, both materials show complete conversion to sodium methoxide. The methoxide is stable on Na_2O even at 598 K. On Na_2O_2, the methoxide begins to decompose at 523 K to form sodium carbonate. All spectra were acquired with a spinning speed of 5 kHz except those at 298 K on Na_2O_2, which were acquired at 2 kHz. All spectra are the result of 512 transients using a 4 s recycle delay.

Superoxides exhibit simple paramagnetism, and this is reflected in the Curie law behavior suggested by the temperature dependencies of the low-temperature phases in Figure 7. Paramagnetic shifts are of two general types,[37] Fermi contact and dipolar. The Fermi contact shift mechanism requires that unpaired electron spin density be delocalized into s orbitals of the observed nucleus. Since the unpaired electron is associated with the superoxide anion, a Fermi contact contribution to the paramagnetic shift of the alkali metal nucleus would require at least a modest covalent contribution to the chemical bonding between the superoxide and alkali metal. The dipolar shift mechanism operates through space; therefore, the nature of the chemical bond (covalent or ionic) is immaterial to its operation. The geometric character of dipolar couplings suggests that their effects should be strongly sensitive to space group symmetry properties. In particular, since dipolar couplings are second-rank tensors that are traceless at high field, purely dipolar paramagnetic shifts should exactly vanish for cubic symmetry with respect to the distribution of paramagnetic species.

As one moves down the periodic table from sodium to cesium, there is a progression in properties that has a direct bearing on the likelihood of a Fermi contact contribution to the paramagnetic shift of the metal nucleus in the alkali metal superoxide. While sodium compounds could plausibly have a modest amount of covalent bonding, cesium compounds will certainly be purely ionic. These expectations concerning the nature of chemical bonding, the relationship between covalent bonding and Fermi contact shifts, and the geometric dependence of through-space dipolar shifts lead to a straightforward explanation of the data in Figure 7. Any paramagnetic shift for cesium superoxide must be purely dipolar in nature. Dipolar couplings have a geometric dependence described by $(3\cos^2\theta - 1)\mathbf{r}^{-3}$, where $\mathbf{r}$ is the vector between the two spins in question (assumed here to be the metal center and the midpoint in O_2^-) and θ is the angle between $\mathbf{r}$ and $g_{||}$ for the unpaired electron. For a superoxide ion, $g_{||}$ should be oriented along the O−O bond vector. In α-CsO_2, the low-temperature tetragonal phase, there are four equatorial superoxide anions ($\theta = 90°$) and two axial superoxide anions ($\theta = 0°$). A simple calculation shows that if the axial and equatorial distances are different, a net paramagnetic dipolar shift will be expected, as we observe for α-CsO_2. For β-CsO_2, the high-temperature cubic phase, this same calculation predicts that there will be no dipolar contribution to the paramagnetic shift, and this is what we observe experimentally.

The behavior of RbO_2 is almost identical to that of CsO_2, and it is hardly surprising that purely ionic bonding and exclusively dipolar paramagnetic shifts are observed for this compound. Both KO_2 and NaO_2 show modest paramagnetic shifts in their high-temperature cubic phases, and the ^{23}Na apparent chemical shift for the high-temperature phase of NaO_2 shows a non-Curie temperature dependence. We speculate that Fermi contact contributions play a role in the paramagnetic shifts observed for KO_2 and NaO_2.

Conclusions

We surveyed the alkali metal NMR properties of the more accessible oxides (M_2O), peroxides (M_2O_2), and superoxides (MO_2) of Li, Na, K, Rb, and Cs. For the oxides and peroxides, the alkali metal NMR spectra were unremarkable and easily understood in the context of their crystal structures. The superoxides exhibited very strong temperature dependencies as a result of the paramagnetic superoxide anion. This effect was characterized in detail for the superoxides of sodium, potassium, rubidium, and cesium. In the case of CsO_2 and RbO_2, the paramagnetic shift is exclusively from the through-space dipolar mechanism, and the geometric dependence of this shift rationalizes the fact that it vanishes for the high-temperature cubic phases. The effects of paramagnetism could easily confound unprepared attempts at the NMR characterization of catalysts containing phases or clusters of alkali metals and oxygen. For example, at 298 K the ^{133}Cs signal of CsO_2 lies 2000 ppm outside the usual chemical shift range for this nucleus, and it can be resolved only with spinning speeds of ca. 10 kHz or higher. The presence of superoxide in mixed phases can also reduce the spin counts for diamagnetic species in those phases, and we had difficulty obtaining the ^{133}Cs spectrum of Cs_2O_2 until we reduced the superoxide content. It may be that the alkali metal NMR characterization of some catalyst samples should be reexamined in light of the findings of the present investigation. The practice of labeling and selling mixtures of Cs_2O_2 and CsO_2 as "Cs_2O" cannot be helpful and should be discouraged. We purchased "Cs_2O" from three chemical vendors, but only Alfa Aesar identified the product as actually being a mixture of the peroxide and superoxide.

A survey of the reaction chemistry of some of the compounds studied here was undertaken using ^{13}C in situ NMR. While the alkali metal oxides, M_2O, showed the expected basic behavior, the peroxides and superoxides react both as bases and as oxidants. The possibility of alkali metal peroxides or superoxides having roles in reactions on catalysts formulated using alkali metal components should be considered. NMR studies of catalysts containing alkali metal oxide phases are increasing in frequency,[39] and the present study could suggest interpretations based on peroxide and superoxide phases.

Acknowledgment. This work was supported by the National Science Foundation (Grant CHE-9528959). Helpful suggestions were made in the course of this work by Prof. J. Lunsford and

Prof. T. Hughbanks at Texas A&M University. The X-ray powder diffraction facilities used in the analysis of the alkali metal peroxides and superoxides were kindly provided by Prof. A. Clearfield.

References and Notes

(1) Hattori, H. *Chem. Rev.* **1995**, *95*, 537.
(2) Minahan, D. M.; Hoflund, G. B. *J. Catal.* **1996**, *158*, 109.
(3) Ukisu, Y.; Sato, S.; Muramatsu, G.; Yoshida, K. *Catal. Lett.* **1991**, *11*, 177.
(4) Ukisu, Y.; Sato, S.; Muramatsu, G.; Yoshida, K. *Catal. Lett.* **1992**, *16*, 11.
(5) Tsuchiya, S.; Takase, S.; Imamura, H. *Chem. Lett.* **1984**, 661.
(6) Noumi, H.; Misumi, T.; Tsuchiya, S. *Chem. Lett.* **1978**, 439.
(7) Hathaway, P. E.; Davis, M. E. *J. Catal.* **1989**, *116*, 263.
(8) Hathaway, P. E.; Davis, M. E. *J. Catal.* **1989**, *116*, 279.
(9) Yashima, T.; Suzuki, H.; Hara, N. *J. Catal.* **1974**, *33*, 486.
(10) Kim, J. C.; Li, H.-X.; Chen, C.-Y.; Davis, M. E. *Microporous Mater.* **1994**, *2*, 413.
(11) Cotton, F. A. In *Progress in Inorganic Chemistry*; Cotton, F. A., Ed.; John Wiley and Sons: New York, 1962; Vol. 4, pp 125−197.
(12) Borgstedt, H. U.; Mathews, C. K. *Applied Chemistry of the Alkali Metals*; Plenum Press: New York, 1987.
(13) Cotton, F. A.; Wilkinson, G. *Advanced Inorganic Chemistry*; 5th ed.; Wiley-Interscience: New York, 1988.
(14) Thompson, J. K.; Kleinberg, J. *J. Am. Chem. Soc.* **1951**, *73*, 1243.
(15) Klein, W.; Armbruster, K.; Jansen, M. *J. Chem. Soc., Chem. Commun.* **1998**, 707.
(16) Bakulina, V. M.; Vol'nov, I. I.; Matveev, V. V.; Zimina, A. N. *Russ. J. Struct. Chem. (Engl. Transl.)* **1966**, *7*, 791.
(17) Simon, A. *Z. Anorg. Allg. Chem.* **1973**, *395*, 301.
(18) Tsai, K.-R.; Harris, P. M.; Lassettre, E. N. *J. Phys. Chem.* **1956**, *60*, 338.
(19) Helms, A.; Klemm, W. *Z. Anorg. Allg. Chem.* **1939**, *242*, 201.
(20) Bell, A.; Pines, A. In *NMR Techniques in Catalysis*; Bell, A., Pines, A., Eds.; Marcel Dekker: New York, 1994.
(21) Schechter, W. H.; Thompson, J. K.; Kleinburg, J. *J. Am. Chem. Soc.* **1949**, *71*, 1816.
(22) Föppl, H. *Z. Anorg. Allg. Chem.* **1957**, *291*, 13.
(23) Dudrarev, V. Y.; Tsentsiper, A. B.; Dobrolyubova, M. S. *Sov. Phys. Crystallogr.* **1974**, *18*, 477.
(24) Carter, G. F.; Margrave, J. L.; Templeton, D. H. *Acta Crystallogr.* **1952**, *5*, 851.
(25) Templeton, D. H.; Dauben, C. A. *J. Am. Chem. Soc.* **1950**, *72*, 2251.
(26) Carter, G. F.; Templeton, D. H. *J. Am. Chem. Soc.* **1953**, *75*, 5247.
(27) Zhdanov, G. S.; Zvonkova, Z. V. *Dokl. Akad. Nauk SSSR* **1952**, *82*, 743.
(28) Haw, J. F.; Nicholas, J. B.; Xu, T.; Beck, L. W.; Ferguson, D. B. *Acc. Chem. Res.* **1996**, *29*, 259.
(29) Haw, J. F.; Richardson, B. R.; Oshiro, I. S.; Lazo, N. L.; Speed, J. A. *J. Am. Chem. Soc.* **1989**, *111*, 2052.
(30) Campbell, G. C.; Crosby, R. C.; Haw, J. F. *J. Magn. Reson.* **1986**, *69*, 191.
(31) Haw, J. F.; Campbell, G. C. *J. Magn. Reson.* **1986**, *66*, 558.
(32) Brough, A. R.; Grey, C. P.; Dobson, C. M. *J. Am. Chem. Soc.* **1993**, *115*, 7318.
(33) Grey, C. P.; Smith, M. E.; Cheetham, A. K.; Dobson, C. M.; Dupree, R. *J. Am. Chem. Soc.* **1990**, *112*, 4670.
(34) Grey, C. P.; Dobson, C. M.; Cheetham, A. K.; Jakeman, R. J. B. *J. Am. Chem. Soc.* **1989**, *111*, 505.
(35) Campbell, G. C.; Haw, J. F. *Inorg. Chem.* **1988**, *27*, 3706.
(36) Campbell, G. C.; Reibenspies, J.; Haw, J. F. *Inorg. Chem.* **1991**, *30*, 171.
(37) Carlin, R. L. *Magnetochemistry*; Springer-Verlag: New York, 1986.
(38) Harris, R. K. *Nuclear Magnetic Resonance Spectroscopy*; John Wiley & Sons: New York, 1986.
(39) Hunger, M.; Schenk, U.; Burger, B.; Weitkamp, J. *Angew. Chem., Int. Ed. Engl.* **1997**, *36*, 2504.